Canadian Science Publishing

ARTICLE

Spatiotemporal modeling of bycatch data: methods and a practical guide through a case study in a Canadian Arctic fishery

Yuan Yan, Eva Cantoni, Chris Field, Margaret Treble, and Joanna Mills Flemming

Abstract: Excess bycatch of marine species during commercial fishing trips is a challenging problem in fishery management worldwide. The aims of this paper are twofold: to introduce methods and provide a practical guide for spatiotemporal modelling of bycatch data, as well as to apply these methods and present a thorough examination of Greenland shark (*Somniosus microcephalus*) bycatch weight in a Canadian Arctic fishery. We introduce the spatially explicit two-part model and offer a step by step guide for applying the model to any form of bycatch data, from data cleaning, exploratory data analysis, variable and model selection, model checking, to results interpretation. We address various problems encountered in decision making and suggest that researchers proceed cautiously and always keep in mind the aims of the analysis when fitting a spatiotemporal model. Results identified spatiotemporal hotspots and indicated month and gear type were key drivers of high bycatch. The importance of onboard observers in providing robust bycatch data was also evident. These findings will help to inform conservation strategies and management decisions, such as limiting access to spatial hotspots, seasonal closures and gear restrictions.

Résumé : Les prises accessoires excédentaires d'espèces marines durant les sorties de pêche commerciale constituent un épineux problème en gestion des pêches partout dans le monde. Le présent article a deux objectifs, à savoir : présenter des méthodes et un guide pratique pour la modélisation spatiotemporelle de données sur les prises accessoires et appliquer ces méthodes et présenter un examen exhaustif du poids des prises accessoires de laimargues atlantiques (*Somniosus microcephalus*) dans une pêche dans l'Arctique canadien. Nous présentons le modèle bipartite spatialement explicite, ainsi qu'un guide par étapes d'application de ce modèle à toute forme de données sur les prises accessoires, du nettoyage des données à l'interprétation des résultats en passant par l'analyse exploratoire des données, la sélection des variables et du modèle et la vérification du modèle. Nous abordons divers problèmes rencontrés dans le processus décisionnel et suggérons que les chercheurs fassent preuve de prudence et gardent toujours en tête les objectifs de l'analyse quand ils calent un modèle spatiotemporel. Les résultats font ressortir des points chauds dans l'espace et le temps et indiquent que le mois et le type d'engin sont les principaux facteurs déterminants de prises accessoires élevées. Ils mettent également en évidence l'importance d'observateurs à bord pour la collecte de données robustes sur les prises accessoires. Ces constatations aideront à éclairer l'élaboration de stratégies de conservation et la prise de décisions de gestion, telles que des restrictions sur l'accès à des points chaudes, des fermetures saisonnières et des restrictions visant certains engins. [Traduit par la Rédaction]

1. Introduction

During commercial fishing trips, various non-target species are often caught unintentionally and usually discarded afterward. These bycatch events sometimes involve vulnerable, long-lived and endangered marine species, such as sharks, whose survival probabilities are low following discard (MacNeil et al. 2012). The problem of excess bycatch is faced by fisheries worldwide and contributes to the broader concern of overfishing (Davies et al. 2009). Therefore, understanding bycatch patterns and their drivers is important for contemporary fisheries management to develop conservation strategies for bycatch reduction.

At-sea observers may be assigned to fishing trips to monitor compliance to fishery regulations and to collect catch and effort data. Data they collect can include weights and (or) counts of every species caught in each haul (fishing tow), as well as locations and dates related to the haul, vessel and gear specification, fishing effort (e.g., tow time and speed for trawl fishing, net length and mesh size for gillnet fishing, number of hooks for longline fishing), and possibly environmental covariates (e.g., sea surface temperature, bathymetry). Such observer data provide a valuable resource for investigating bycatch patterns.

Statistical models are at the heart of modern data analysis and aim at extracting information from noisy data. Catch count or weight data, for example, can be regarded as random samples drawn from the underlying population of the species in quantity or biomass, respectively. To infer the underlying population distribution, possibly changing through time and across space, from the available catch data, proper statistical models are needed to remove factors affecting catches other than abundance. For example, these could be factors that affect catchability and availability. Generalized linear models (GLMs) are widely used in stock assessments for catch per unit effort (CPUE) standardization and derivation of abundance or biomass indices (Gavaris 1980; Guisan et al. 2002). GLMs decompose

Received 15 July 2020. Accepted 27 May 2021.

Y. Yan, C. Field, and J.M. Flemming. Department of Mathematics & Statistics, Dalhousie University, Halifax, NS B3H 4R2, Canada.
E. Cantoni. Research Center for Statistics and Geneva School of Economics and Management, University of Geneva, Geneva, Switzerland.
M. Treble. Fisheries and Oceans Canada, Winnipeg, MB R3T 2N6, Canada.

Corresponding author: Yuan Yan (email: yuan.yan@dal.ca).

catch variability into contributions from different factors, such as gear type, environmental conditions (e.g., temperature, salinity), fishing season and region as well as possible interaction terms. Furthermore, by treating some factor(s) as random effects, the GLMs are extended to generalized linear mixed models (GLMMs). Maunder and Punt (2004) provide a nice review of the early approaches using GLMs and GLMMs to standardize catch and effort data. Often, spatial information on fishing hauls is used coarsely to group hauls by geographical regions and incorporated in the analysis of catch data by treating these regions as fixed effects in a GLM (Lo et al. 1992; Campbell 2004) or as independent and identically distributed (i.i.d.) random effects in a GLMM (Ortiz and Arocha 2004; Thorson and Ward 2013). Additionally, including fishing trips as i.i.d. random effects in GLMMs not only accounts for vessel variability, but also implicitly captures spatiotemporal interactions, because fishing trips are often clustered in space and time (Helser et al. 2004; Cantoni et al. 2017). Recently, especially with accurate records of fishing location, more sophisticated models that include spatial or spatiotemporal components via latent stochastic processes are becoming popular in fisheries science (Nishida and Chen 2004; Sims et al. 2008). Adding spatially and (or) spatiotemporally correlated random effects into a GLM results in more efficient use of available data (Thorson et al. 2015) and can shed light on the spatiotemporal dynamics of the underlying population density (Carson et al. 2017).

Bycatch data for certain species, especially rare ones, are characterized by a large number of zeros resulting from the absence of the species in most hauls. Previous studies of bycatch count data have tended to use either the zero-inflated version of the Poisson and negative binomial model (Cosandey-Godin et al. 2015) or the hurdle model (Cantoni et al. 2017) to deal with the excess of zeros. The two-part model is the counterpart of the hurdle model for non-negative continuous data (rather than count data) with a cluster at zero, or so-called semicontinuous data. Sometimes the term "two-part model" refers to models for both semicontinuous data and the hurdle model for count data (Zuur et al. 2009, Chapter 11), or even more broadly including zero-inflated models. In this paper, we use the "two-part model" in the narrow sense referring to a two-part semicontinuous model. The hurdle model and the two-part model have the advantage of separating the presence/absence process from the process influencing the size conditional on the presence. Min and Agresti (2002) provide a review of models dealing with nonnegative data with clumping at zero for both count and semicontinuous data. In fisheries, the hurdle model and the two-part model are referred collectively as delta-distributions (Lo et al. 1992), with the "delta" in the sense of the Dirac delta function because a point mass is placed at zero. The delta-lognormal, delta-gamma, or more generally the delta-GLMM (Ortiz and Arocha 2004) have also been adopted for analysing catch-rate data from fishery independent surveys, because they share with bycatch data the feature that a large proportion of hauls will have zero catch for certain species (Helser et al. 2004). Shelton et al. (2014) and Thorson et al. (2015) extended the delta-GLMM by adding spatial random effects at given knots using a geostatistical model to yield more accurate indices of abundance from survey data.

Even though spatial two-part models have become popular in fisheries science in recent years and been applied to analyse both catch data from fishery-independent surveys and bycatch data from commercial fishing trips, the purposes of the analyses are different. The main goal for analysing survey data is to estimate species distribution in space-time and extract a yearly index of abundance. On the other hand, for bycatch data, the primary concerns are to determine factors that affect bycatch to avoid them, and ultimately to establish effective management and conservation decisions, such as gear restrictions, catch quotas, seasonal closures and limiting access to spatial hotspots. In previous applications, essential details for using spatial two-part models were usually omitted and practitioners may find it difficult to apply these methods to their own data. In this paper we consider the data analysis steps from data cleaning to results interpretation with emphasis on potential problems when fitting spatial two-part models.

We analyse observer data from a Canadian Arctic Greenland halibut (*Reinhardtius hippoglossoides*) fishery and focus on the bycatch species of Greenland shark (*Somniosus microcephalus*), which is the world's oldest vertebrate (Nielsen et al. 2016) and vulnerable to the bycatch problem. The aim of the analysis is to understand bycatch risk for Greenland shark by identifying driving factors and spatial patterns of bycatch occurrence (and its magnitude). We consider a two-part model with latent Gaussian random fields as spatial random effects in both parts. The dataset, R codes, and associated.cpp files are all available online in the online Supplements[1].

2. Materials and methods

2.1. Data preparation

Observer data provided by Fisheries and Oceans Canada (DFO) are records of fishing trips conducted by Nunavut and Newfoundland fishing companies for Greenland halibut inside the Northwest Atlantic Fisheries Organization Subarea 0, for years 2013 to 2017. The fishing area ranges from Davis Strait to southern Baffin Bay, which connects Nunavut's Baffin Island and Greenland and serves as the only large-scale industrial finfish fishery in the Canadian Arctic. Figure 1*a* shows geographical features of the fishing area. The map was created in the R software (R Core Team 2021) using the marmap package (Pante and Simon-Bouhet 2013). In this area, Greenland sharks are commonly caught as bycatch and discarded (MacNeil et al. 2012). The complete dataset contains information on all gear types, mainly from trawl and gillnet fleets. An initial examination of the data reveals that bycatch incidence rate for Greenland shark is much higher for the trawl fleet (892 out of 3596 hauls, 24.8%) than the gillnet fleet (77 out of 3299 hauls, 2.3%). Additionally, 100% observer coverage (every trip has an observer) is required by DFO for factory trawlers operating in this fishery due to their fishing power and capacity to process at sea. Therefore, we focus on Greenland shark bycatch from the trawl fleet because these contain the bulk of the bycatch. Practitioners should be aware that many fisheries do not have this high level of observer coverage and that fishery-dependent data without an observer on board can be incomplete (Benoît and Allard 2009; Graham et al. 2011; Curtis and Carretta 2020).

The 3596 hauls came from 54 fishing trips. Trip specific information includes vessel class based on gross registered tonnage (two levels: 500–999.9 and >2000 t, there were no vessels between 1000 and 1999.9 t). For each haul within a fishing trip, catches were sorted by species and then kept weight and discard weight for every species are recorded. We took the sum of the kept and discard weight of Greenland halibut as target weight and use discard weight of Greenland shark as bycatch weight because all were discarded. In addition, along with each haul, the start and end locations and dates, average fishing depth, tow time (duration of a tow), gear specification (two levels: single bottom trawl and twin bottom trawl) and source of the record are also provided. The source indicates whether the observer based their assessment of the catch on personal observation or information provided by the captain or his designate (e.g., when the observer was taking a break and not able to personally observe every haul). Overall, the records by non-observers comprise 10.7%.

[1]Supplementary data are available with the article at https://doi.org/10.1139/cjfas-2020-0267.

Fig. 1. Summary of the Greenland shark bycatch data: (*a*) fishing area with isobathymetric lines and locations of the 3596 hauls shown by dots (indicating bycatch absent from the haul) and plus signs (indicating bycatch present in the haul), with different colours representing the 54 fishing trips associated with the hauls (map created in R using the marmap package); (*b*) hauls with bycatch occurrence among total hauls by year; (*c*) bycatch and target weight by year. [Colour online.]

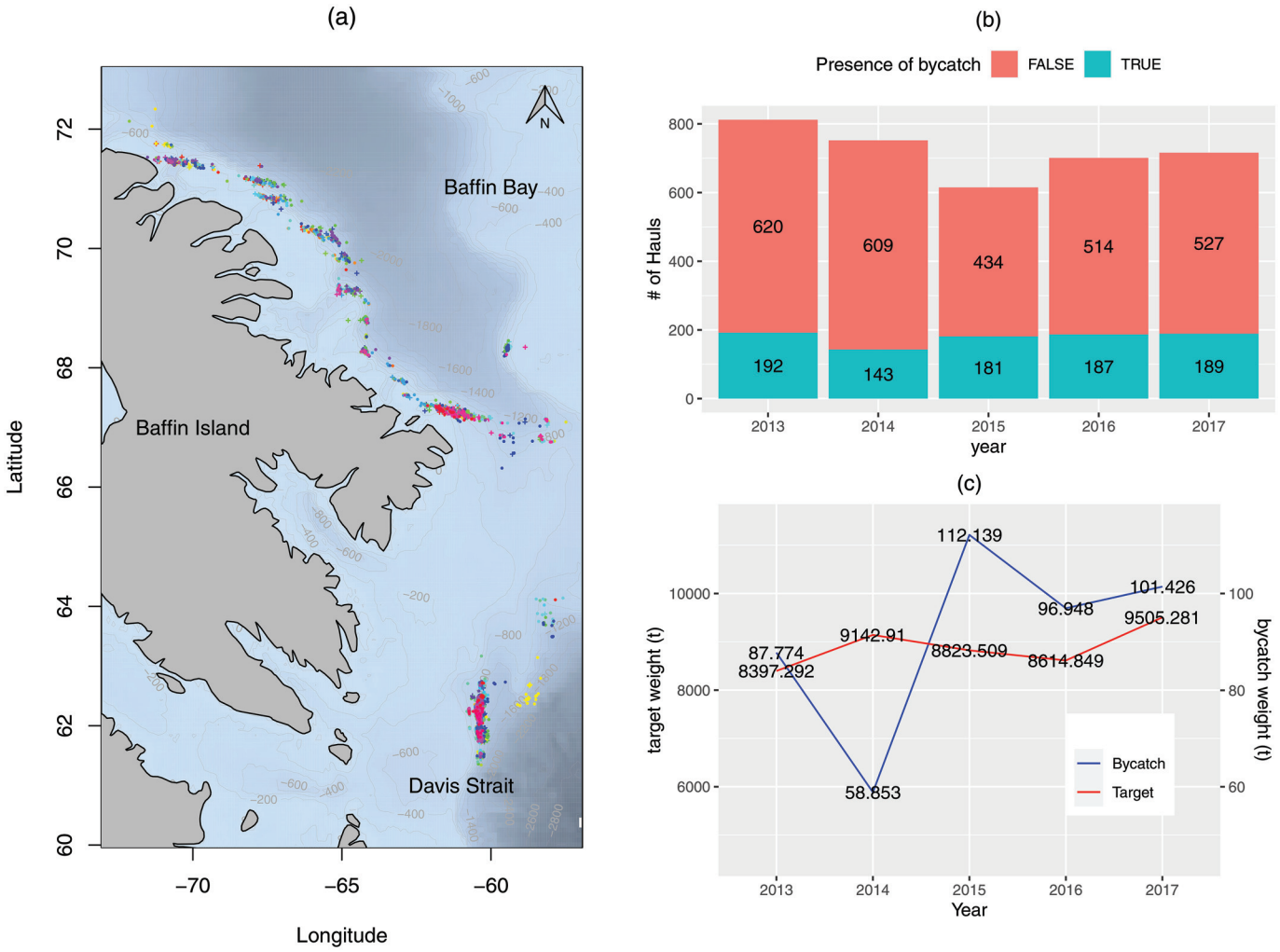

Because data may be inputted manually from records on paper or directly into computers, errors are unavoidable. Therefore, data cleaning is an important first step to prepare the raw data for further analysis. By plotting the start and end fishing longitude and latitude in the raw data, we found some locations to be on shore or far away from other hauls within the same trip. Details can be found in Fig. S1 of the Supplementary materials[1]. We identified and corrected these erroneous locations one by one according to some sensible assessments (e.g., mistaken 6 as 5, 2 as 7). Then the mid point of the start and end locations were taken as the location associated with each haul. We also noticed some hauls with unreasonably large bycatch weights of Greenland shark (6–41 t), all of which came from two particular fishing trips. After checking the original paper files, we were able to determine that these extreme bycatch weights were caused by a key punching problem (with an extra zero added) and we fixed those weight records accordingly. When this kind of error is hard to solve, the winsorization procedure we introduce later under methods can help to reduce the influence of erroneous data points and achieve robustness.

Following the data cleaning step, exploratory data analysis (EDA) is important to reveal some key features of the data. Table 1 provides the number of hauls with or without bycatch for the three two-level factors, i.e., source, vessel class and gear. We also notice that there are very few hauls from smaller vessels (500–999.9 t) and none of them have bycatch. Figure 1 provides a visual summary of the data after pre-processing. Figure 1*a* shows the 3596 haul locations labeled by dot or plus sign, with plus sign indicating presence of Greenland shark bycatch. The hauls are grouped by the 54 fishing trips represented by different colours, from which we can see the trips are clustered in space, as

Table 1. Summary of the three two-level factors (source, vessel tonnage and gear) with respect to the total number of hauls, as well as the number of hauls without Greenland shark bycatch and positive bycatch weight, respectively.

	No. of hauls					
	Source		Vessel (t)		Gear	
	Observer	Non-observer	500–999.9	>2000	Single trawl	Twin trawl
Bycatch absent	2384	320	24	2680	1088	1616
Bycatch > 0	827	65	0	892	314	578
Total	3211	385	24	3572	1402	2194

expected. As shown in Figs. 1*b* and 1*c*, the number of hauls with Greenland shark bycatch among total haul numbers in each year shows a persistent and stable bycatch occurrence, while bycatch weights vary quite a lot through years, e.g., bycatch weight in 2015 almost doubles that of 2014. More results for EDA following protocol of Zuur et al. (2010) can be found in Figs. S2–S4 of the Supplementary materials[1].

2.2. Methods

Recorded bycatch weights can be affected by various factors, such as measurement skill (e.g., source of the record), catchability (e.g., fishing effort), in addition to the underlying distribution of Greenland shark bycatch in space and time. Methods should be devised keeping in mind the goal of the analysis. To understand driving factors for Greenland shark bycatch and extract information about the spatial distribution of the bycatch, it is crucial to include a stochastic spatial component in the model. The Gaussian random field is a popular geostatistical tool for stochastic spatial processes, because it is fully characterized by its mean and covariance function. We considered a two-part model with latent Gaussian random fields as spatial random effects in both parts for analysing the Greenland shark bycatch data. A first step to incorporating the spatial information is to project the latitude and longitude of the fishing locations onto a plane. We used the WGS84 – UTM zone 19 N coordinate reference system, which is appropriate for the Canadian Arctic region. The new coordinates were in unit of kilometres. We let y_i denote the Greenland shark bycatch weight from the ith haul, at projected fishing location $\boldsymbol{s}_i$, $i = 1, \ldots, n$, where n is the total number of hauls.

The first part models the incidence of Greenland shark bycatch using a binary GLMM with canonical logit link (logistic regression):

$$(1)\qquad \begin{aligned} &\text{logit}\{\mathbb{P}(y_i > 0)\} = \text{logit}\{p_i\} = x_i^{\mathrm{T}}\beta^{(p)} + \xi^{(p)}(\boldsymbol{s}_i) \\ &\mathbb{1}(y_i > 0) \sim \text{Bernoulli}(p_i) \end{aligned}$$

while the second part uses a gamma GLMM with log link for positive bycatch weight:

$$(2)\qquad \begin{aligned} &\log\{\mathbb{E}(y_i|y_i > 0)\} = \log\{\lambda_i\} = x_i^{\mathrm{T}}\beta^{(\lambda)} + \xi^{(\lambda)}(\boldsymbol{s}_i) \\ &y_i|y_i > 0 \sim \text{gamma}\left(\sigma_G^{-2}, \lambda_i\sigma_G^2\right) \end{aligned}$$

where $\boldsymbol{x}_i$ is a vector of covariates, $\beta^{(p)}$ and $\beta^{(\lambda)}$ are fixed effect coefficients for the two parts, $\xi^{(p)}(\boldsymbol{s})$ and $\xi^{(\lambda)}(\boldsymbol{s})$ are two independent Gaussian random fields indexed by s in continuous space, $\xi^{(p)}(\boldsymbol{s}_i)$ and $\xi^{(\lambda)}(\boldsymbol{s}_i)$ for $i = 1, \ldots, n$ can be regarded as multivariate realizations from the corresponding random fields; gamma(a, b) denotes the gamma distribution with shape parameter a and scale parameter b, and σ_G^2 is the dispersion parameter.

The log link used in the second part of the model transforms the multiplicative relationship between catches and covariates in a catch equation (Campbell 2004) into an additive one. Moreover, the gamma distribution is suitable when the standard deviation grows proportionally to the mean, with $\mathbb{E}(y_i|y_i > 0) = \lambda_i$ and $\text{Var}(y_i|y_i > 0) = \lambda_i^2\sigma_G^2$, as suggested by plotting the positive bycatch weights against the log target weights (see Fig. S5 in the Supplementary materials[1]). Another popular choice for the positive part is the lognormal distribution. By checking visually whether the plot of positive bycatch weights in log scale against the log target weights follows assumptions of a simple linear model, we found the lognormal distribution unsuitable for our bycatch weights data.

The two Gaussian random fields were modeled with mean 0 and parametric isotropic covariance functions $C(d;\boldsymbol{\theta}^{(p)})$ and $C(d;\boldsymbol{\theta}^{(\lambda)})$, where d is the distance between two locations. A popular choice for the parametric covariance function is the Matérn covariance function, which takes the following form:

$$C(d;\boldsymbol{q}) = \frac{\sigma^2}{\Gamma(\nu)2^{\nu-1}}\left(\frac{d}{\phi}\right)^{\nu}K_\nu\left(\frac{d}{\phi}\right)$$

where $\boldsymbol{q} = (\sigma^2, \phi, \nu)^{\top}$, σ^2 is the variance of the random field, $\phi > 0$ is the range parameter, $\nu > 0$ controls the smoothness (mean square differentiability) of the spatial process, and K_ν is the modified Bessel function of the second kind of order ν. The commonly used exponential covariance, $C(d;\sigma^2,\phi) = \sigma^2\exp(-d/\phi)$, is a special case of the Matérn family with $\nu = 0.5$; while the Gaussian covariance function, $C(d;\sigma^2,\phi) = \sigma^2\exp(-\frac{d^2}{\phi^2})$ is a special case of the Matérn family as $\nu \to \infty$ (Stein 1999).

Assuming the two parts are independent, parameters for each can be estimated separately. We argue that the independence assumption is appropriate in this scenario because factors that affect incidence of bycatch (e.g., wide distribution and long distance migration; Campana et al. 2015; Nielsen et al. 2014) and weight (e.g., variability in size and density; MacNeil et al. 2012; Rusyaev and Orlov 2013) can be very different. If this is not the case, the correlated two parts can be modelled jointly (Cantoni et al. 2017).

2.3. Computational aspects

With a sample size of $n = 3596$ for bycatch occurrence (binary part) and $n = 892$ for positive bycatch weight (gamma part), the two-part model with latent Gaussian random fields faces two computational challenges for parameter estimation and prediction of bycatch weight at unobserved locations. These challenges are common in fisheries science when analysing catch data with more than a few hundreds records.

The first issue comes from the need to invert an $n \times n$ covariance matrix for calculating a multivariate Gaussian density. The partial realization of $\xi^{(\cdot)}(s)$, with the dot $(\cdot)$ standing for either p or λ, at the n observed locations follows a multivariate Gaussian distribution, $\boldsymbol{\xi}^{(\cdot)} = \left[\xi^{(\cdot)}(s_1), \ldots, \xi^{(\cdot)}(s_n)\right]^{\mathrm{T}} \sim \mathcal{N}(0, \boldsymbol{\Sigma}_\xi^{(\cdot)})$, with the $n \times n$ covariance matrix $\boldsymbol{\Sigma}_\xi^{(\cdot)}$ determined by the covariance function $C(d;\theta_\xi^{(\cdot)})$ and the $n \times n$ distance matrix $\mathbf{D}$ of the n observed locations. To deal with this problem, we use a Gaussian Markov Random Field (GMRF) at discrete locations with sparse precision matrix (the inverse of a covariance matrix), to represent the continuously indexed Gaussian random field via stochastic partial differential equations (SPDE) (Lindgren et al. 2011). In essence, it is the direct sparse modelling of the precision matrix in GMRF (instead of the covariance matrix) that makes it computationally feasible. To implement this approximation, a mesh is created, which is a triangulation of the spatial domain with vertices (knots) near the data locations and some extra locations such that the minimum edge length is larger than a cut-off value for efficiency and the maximum edge length does not exceed a prescribed level for better approximation. The Gaussian random field can be approximated by the GMRF at the mesh with precision matrix $\mathbf{Q}$ if $\mathbf{Q}^{-1}$ is close to $\boldsymbol{\Sigma}$ (in some norm), where $\boldsymbol{\Sigma}$ is the covariance matrix of the Gaussian random field at the mesh locations. Parameters involved in the SPDE approach for the precision matrix $\mathbf{Q}$ are α, κ and τ. They are related to the Matérn covariance function by $\alpha = \nu + d/2$, $\kappa = 1/\phi$, which results in an effective range of $\sqrt{8\nu}/\kappa$ (distance at which the correlation decreases to about 0.1):

$$\tau^2 = \frac{\Gamma(\nu)\phi^{2\nu}}{\Gamma(\nu + d/2)(4\pi)^{d/2}\sigma^2}$$

where d is the dimension. α cannot be estimated and is usually fixed based on prior knowledge of the smoothness of the process. Nevertheless, the choice of α does not affect the results substantially and so we fix α at 2 in our implementation.

Fig. 2. Visualization of problems in abandoned models: (*a*) linear predictor of the binary part by the summation of depth, year, month and the spatial random effects of our spatial GLMM including tow time as a covariate; (*b*) corresponding fixed effects of tow time for the binary part at the logit scale; (*c*) predicted spatial random effects at mesh locations for the gamma part of our spatial GLMM with winsorized bycatch weights. [Colour online.]

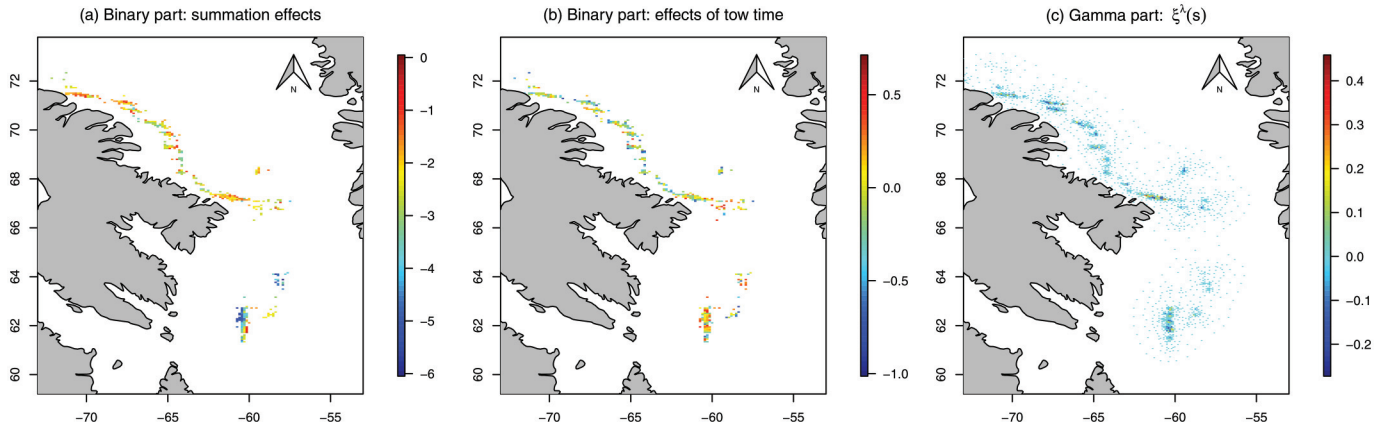

The second issue is related to the high-dimensional integration involved in the likelihood of a GLMM because random effects need to be integrated out. For Gaussian models with normally distributed random effects, the integral remains Gaussian, however, non-Gaussian GLMMs are not subject to this simplification by marginalization. Markov chain Monte Carlo (MCMC) methods are customarily used to approximate such integrals, especially within the Bayesian framework. However, MCMC methods require high computational power and sometimes encounter convergence and mixing problems. The Template Model Builder (TMB) package (Kristensen et al. 2016) in the R software computes the integral via the Laplace approximation and utilizes automatic differentiation (Griewank and Walther 2008) to assist optimization to obtain a maximum likelihood estimator (MLE). Empirical evidence shows good performance of the Laplace approximation for dealing with non-Gaussian distributions (Kristensen et al. 2016). TMB also conveniently supports the SPDE approach for approximating the Gaussian random field. Therefore, our models are fitted using the TMB package in R. Alternatively, one could fit with the VAST package, which is a wrapper using the TMB and SPDE packages; see Thorson (2019) for its usage.

2.4. Variable selection and model comparison

2.4.1. *Variable selection*

We first fitted the binary part of our spatial two-part model in eq. 1 with all covariates included. Figures S2–S4 of the Supplementary materials[1] summarize the covariates. We took logarithm of target weight so that it was in the same unit as bycatch weight in log link. Based on scatterplots of the covariates versus the response variable in Fig. S2[1], we decided how continuous covariates enter the model. Usually, depth enters the model in both linear and quadratic terms, however, a parabolic effect of depth to bycatch weight is not obvious in Fig. S2[1]. Moreover, when depth range is limited due to fishery locations, a linear relationship is sufficient. The three continuous covariates, target weight in log scale, tow time and average fishing depth were centered and scaled. For categorical variables, there are 5 years and 11 months (no haul from March) for temporal factors, with 2013 and January as reference levels. For factors of vessel, gear, and source, all of which have two levels, the vessel larger than 2000 t, single trawl, and observer are set as reference levels, respectively. Those covariates affect bycatch in different ways and interpretation of the effects is crucial. Because the trawlers take hauls from the sea bottom, the average fishing depth is the average bathymetry during the fishing trip and can be regarded as an environmental factor that influences the density or spatial distribution of Greenland shark bycatch. Haul year and month enter our model as factors to capture temporal variability. The total effects of depth, year, month and the spatial random effect can be interpreted as the underlying spatiotemporal distribution of Greenland shark bycatch. Tow time, target weight in log scale, gear and vessel types are all related to fishing effort and affect catchability of Greenland shark. Effects related to source of the record can be interpreted as measurement skill and capture possible differences in weight estimation between observers and non-observers given true bycatch weight. When interpreting results it is important to distinguish between coefficients that affect density or abundance of the bycatch species such as depth or habitat features (density covariates), from those that affect the ability to catch them, such as tow time or gear type (catchability covariates) (Thorson 2019). Including catchability factors could reduce variation, which would lead to more precise results. Also, catchability factors can often be considered for use by resource managers to mitigate or control bycatch.

It is important to examine whether the fitted results are consistent with previous knowledge and to check for suspicious patterns before conclusions can be drawn. Spatial plots of the linear predictor for the binary part by the summation of depth, year, month and the spatial random effect (Fig. 2*a*) along with the fixed effects of tow time (Fig. 2*b*), show a dubious pattern in that they contribute to the predictor in opposite directions. Comparing the estimated fixed effect coefficients with GLM fit without spatial random fields reveals that adding spatial effects causes the coefficient for tow time to increase dramatically from 0.04 to 0.28. We suspected there is some spatial confounding because duration of tows were not randomly distributed in space, which may depend on bottom smoothness, with tow time longer for flatter surface and shorter under rough conditions. Bearing in mind the goal of the analysis is to disentangle spatiotemporal effects in bycatch distribution of Greenland shark from factors affecting catchability, and, in addition, that tow time and target weight are both measures of fishing effort and are strongly correlated, we dropped tow time from the binary part to avoid confounding.

For the positive bycatch weights, there are a few hauls with extremely high records. To reduce the influence of these unusual weights on model fitting, we first winsorized the bycatch weights. Winsorization sets the extreme values to some threshold value thereby down-weighting them appropriately rather

Fig. 3. Receiver operating characteristic (ROC) curves of predicting bycatch occurrence from the GLM, GLMM with trip as random effects and spatial GLMM for both training and testing sets in 5-fold cross-validation. [Colour online.]

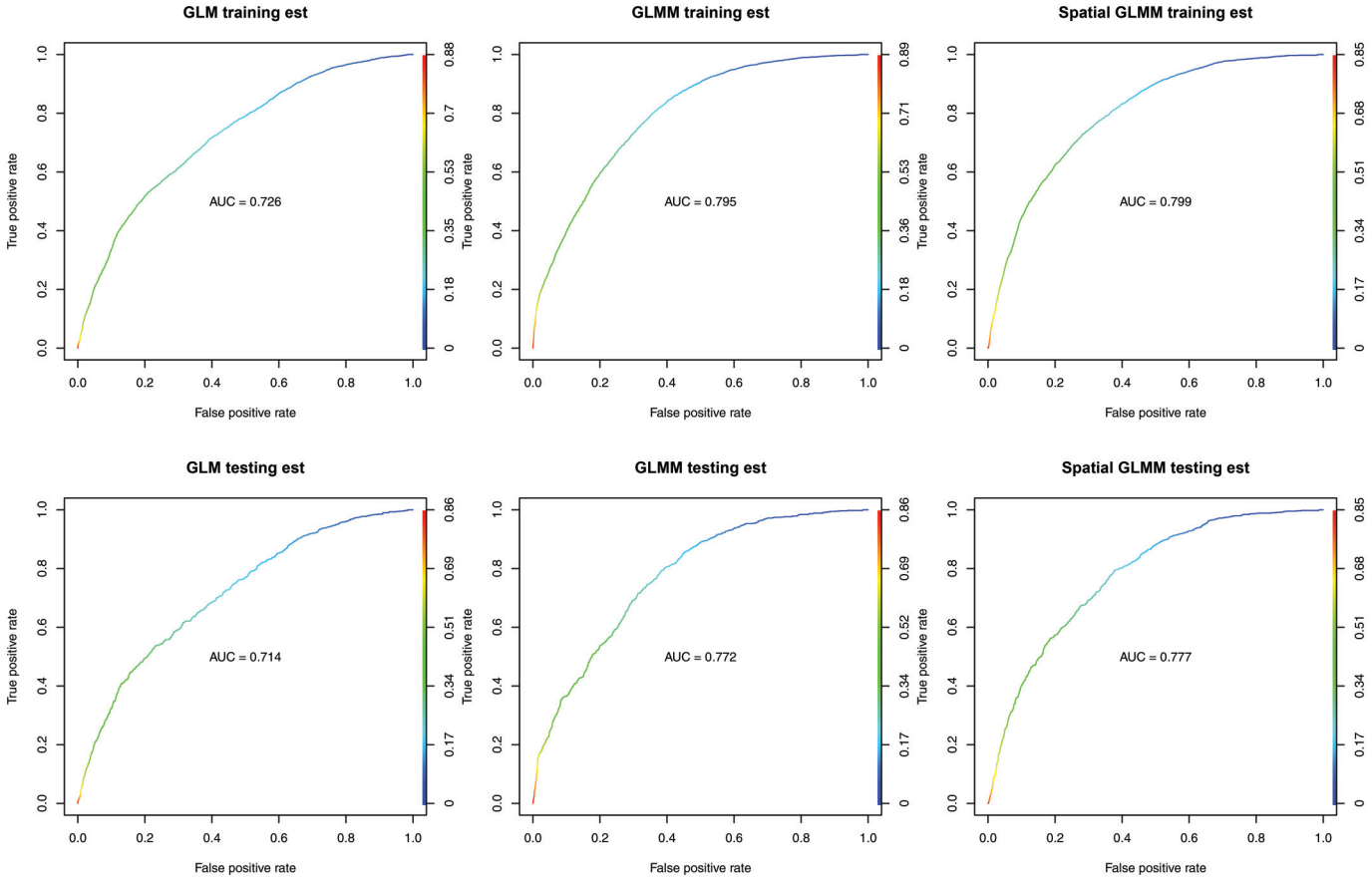

than removing them entirely. Instead of using a conventional percentile like 95%, we set the cutoff value based on outliers from the adjusted boxplot (Hubert and Vandervieren 2008) of bycatch weights, because the bycatch weights are highly skewed. The largest three records, 4100, 3750 and 3745 kg were all winsorized to 3013.5 kg, which is the upper fence of the adjusted boxplot (see Fig. S6 in the Supplementary materials[1]). There were also 25 small weight values were winsorized to the lower fence based on the adjusted boxplot. Next, we fitted the gamma part of our spatial model in eq. 1. Because all hauls with positive bycatch weight were from vessels larger than 2000 t, the vessel factor was dropped. The predicted random field (Fig. 2*c*) does not show an obvious spatial pattern but rather some tiny isolated "hotspots" and "valleys". This is because the estimated effective range of the random field is 2.9 km, far too small when compared to the spatial range of the data. Consequently, the spatial random field in the gamma part cannot improve the model in terms of interpretability.

2.4.2. Model comparison

We believe the ultimate goal of model fitting is to gain insights into the process(es) being modelled. Therefore, we used 5-fold cross-validation to compare the spatial two-part model (spatial GLMM) with a two-part model without random effects (GLM) and one using trip as random effects (GLMM) based on their predictive performance. Note that prediction with GLMM for a new trip is limited to the fixed effect, and cannot borrow information from nearby observations. For a fair comparison with the GLMM, training sets were carefully chosen to include all 54 trips, so that no "new" trip appeared in the testing set. Practitioners can simply resample until trips in the training set contain all trips in the testing set (Cantoni et al. 2017).

For the binary part, we used the predicted occurrence rate $\hat{p}_i$ as a classifier and evaluated the predictive performance using area under the receiver operating characteristic (ROC) curve (AUC). The ROC curve is a plot of the true positive rate (TPR, also known as power–sensitivity–recall) against the false positive rate (FPR, also known as type I error–fall-out–specificity) for a binary predictor with varying threshold. The related null hypothesis is "bycatch absent" and the type I error or false positive is to predict bycatch occurs when it is actually absent. For example, we predict the ith haul present with Greenland shark bycatch if $\hat{p}_i$ is larger than the threshold. With a low threshold value, more hauls will be predicted with bycatch present and results in high values for both TPR and FPR. For a good predictor, we expect high TPR while keeping the FPR low. So the closer the curve is to the top left corner, the better the prediction. AUC provides a summary statistic for the ROC curve, with a higher value indicating better overall predictive performance. Figure 3 shows ROC curves of predicting bycatch occurrence using the three models for both training and testing sets in 5-fold cross-validation using the ROCR package (Sing et al. 2005). The coloured legend on the right of each plot corresponds to the threshold value that contributes to a TPR–FPR point with the colour on the ROC curve. For all three models, the AUC for the testing set is similar to the training set, suggesting genuine predictive ability. Our spatial GLMM performed best among the three. Even though the improvement of the spatial GLMM over the GLMM was not enormous comparing the AUC values, the spatial model has the advantages of

Fig. 4. Histograms of the response residuals for gamma part by the GLM, GLMM with trip as random effects and spatial GLMM for both training and testing sets in 5-fold cross-validation.

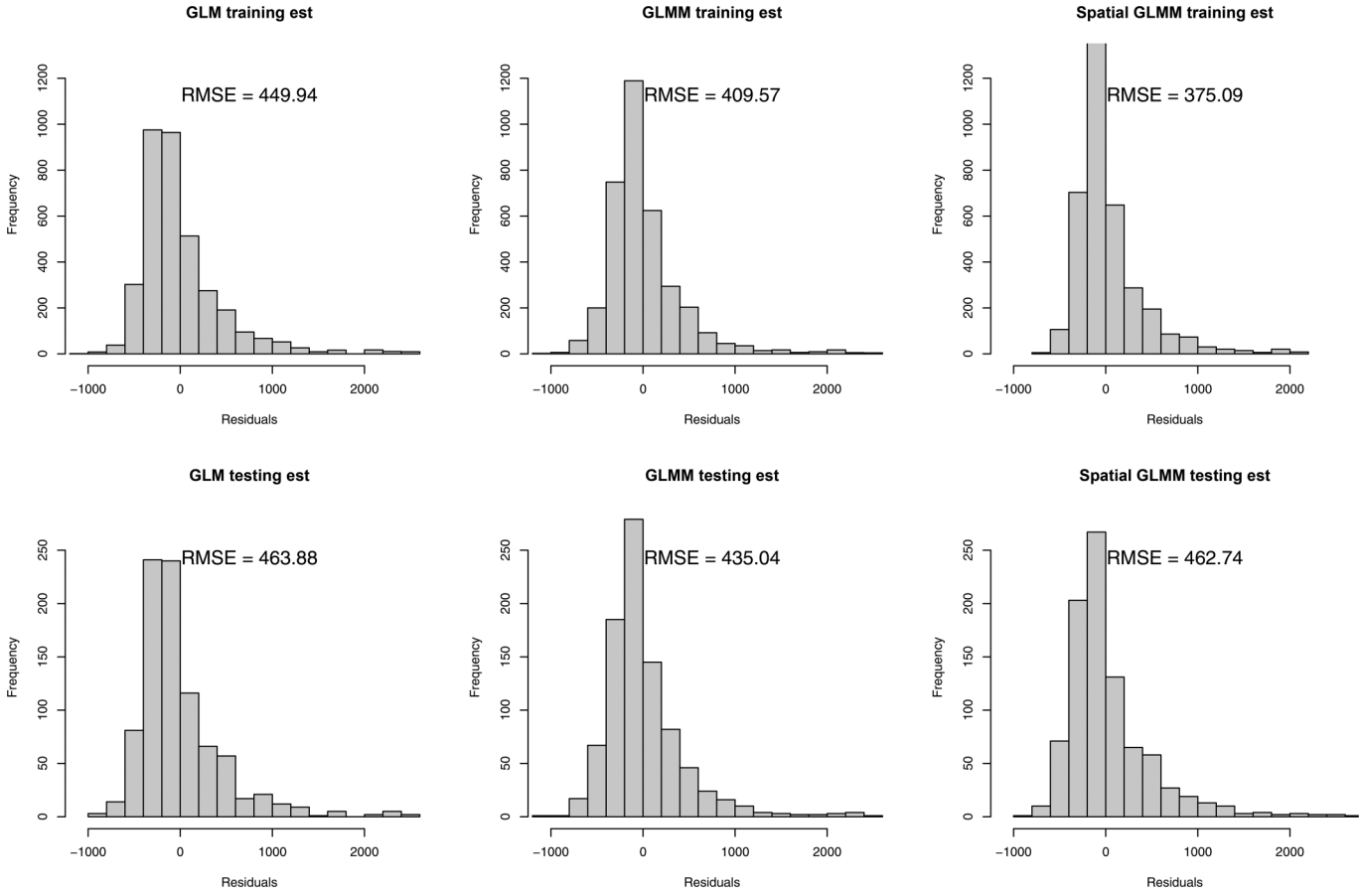

capturing the spatial patterns explicitly as well as enabling prediction at unobserved locations.

For the gamma part, we used root mean square error (RMSE) to evaluate predictive performance. Figure 4 presents histograms of the response residuals along with the RMSE in 5-fold cross-validation using the three models. For the spatial model, there was a big difference in RMSE between the training and testing set, which indicated an overfitting problem and that predictive ability would not extend to a new dataset. Hence we concluded that the sporadic hotspots shown in the estimated random fields for the gamma part of our spatial GLMM (Fig. 2*c*) were artifacts of overfitting. On the other hand, the GLMM using trips as random effects greatly improved the predictive performance from the simple GLM and with stable RMSE between training and testing sets. An explanation for the superior performance of the gamma GLMM for bycatch weight might be that vessels employed in different fishing trips have factors affecting fishing power beyond the specification of tonnage. Using trips as random effects captured this variability in trips due to characteristics of vessels as samples from a larger pool of industry vessels (Helser et al. 2004). However, because trips are clustered in space, variability in vessels may also be mixed with spatial patterns.

2.4.3. Final model

From the cross-validation performance, we selected the spatial GLMM for the binary part and gamma GLMM using trips as random effects for positive bycatch weight as our final model. That is, for Greenland shark bycatch weight y_i from the ith haul, at a projected fishing location $\boldsymbol{s}_i$:

$$\mathbb{1}(y_i > 0) \sim \text{Bernoulli}(p_i),\ \text{logit}\{p_i\} = x_i^{\mathrm{T}}\beta^{(p)} + \xi(\boldsymbol{s}_i),$$
$$\boldsymbol{\xi} \sim \mathcal{N}(\mathbf{0}, \sigma^2\boldsymbol{\Sigma}(\phi))$$
$$y_i | y_i > 0 \sim \text{gamma}\left(\sigma_G^{-2}, \lambda_i\sigma_G^2\right),$$
$$\log\{\lambda_i\} = x_i^{\mathrm{T}}\beta^{(\lambda)} + r_{v(i)},\ r_v \overset{\text{i.i.d.}}{\sim} \mathcal{N}(0, \sigma_v^2)$$

where $\boldsymbol{\xi} = [\xi(s_1), \ldots, \xi(s_n)]^{\mathrm{T}}$, $\boldsymbol{\Sigma}(\phi)$ is the correlation matrix as a function of the range parameter ϕ, and $v(i)$ denotes the trip associated with the ith haul. Residual diagnostics by the simulation-based scaled residuals (Shepherd et al. 2016) using the DHARMa package (Hartig 2020) for both parts can be found in Figs. S7–S8 of the Supplementary materials[1], which do not show obvious violation of the model assumptions.

3. Results

The estimated fixed effect coefficients are shown in Table 2. For the binary part, the target weight (in log scale) has a positive coefficient for predicting presence of bycatch, while fishing depth contributes negatively. The coefficient for gear means the probability of catching Greenland sharks is higher using twin trawl than single trawl. The coefficient of vessel effect is large in absolute value, however, with a highly inflated standard error. This is due to the fact that there are only 24 hauls (all from the same trip) from a vessel in the tonnage category 500–999.9 t and none of them contains Greenland shark bycatch. For the gamma part, fishing depth is again negatively correlated to the positive bycatch weights. However, target weight is not significantly useful in predicting bycatch weights. The source factor is

Table 2. Estimated coefficients of fixed effects and standard errors for the two-part model, with significant effects shown in bold.

		Intercept	Target weight	Tow time	Fishing depth	Gear	Vessel	Source
Binary	Estimate	1.100	**0.365**	—	**−0.254**	**0.518**	−13.893	**−0.746**
	SE	(0.681)	(0.060)	—	(0.084)	(0.110)	(2200.995)	(0.157)
Gamma	Estimate	**6.494**	0.029	0.034	**−0.111**	0.061	—	**−0.203**
	SE	(0.485)	(0.041)	(0.036)	(0.039)	(0.068)	—	(0.094)

Fig. 5. Spatial plots of the latent Gaussian random fields, month, year and depth effects, as well as their summation as the underlying distribution of Greenland shark bycatch occurrence on the linear predictor scale for the binary part of the model. [Colour online.]

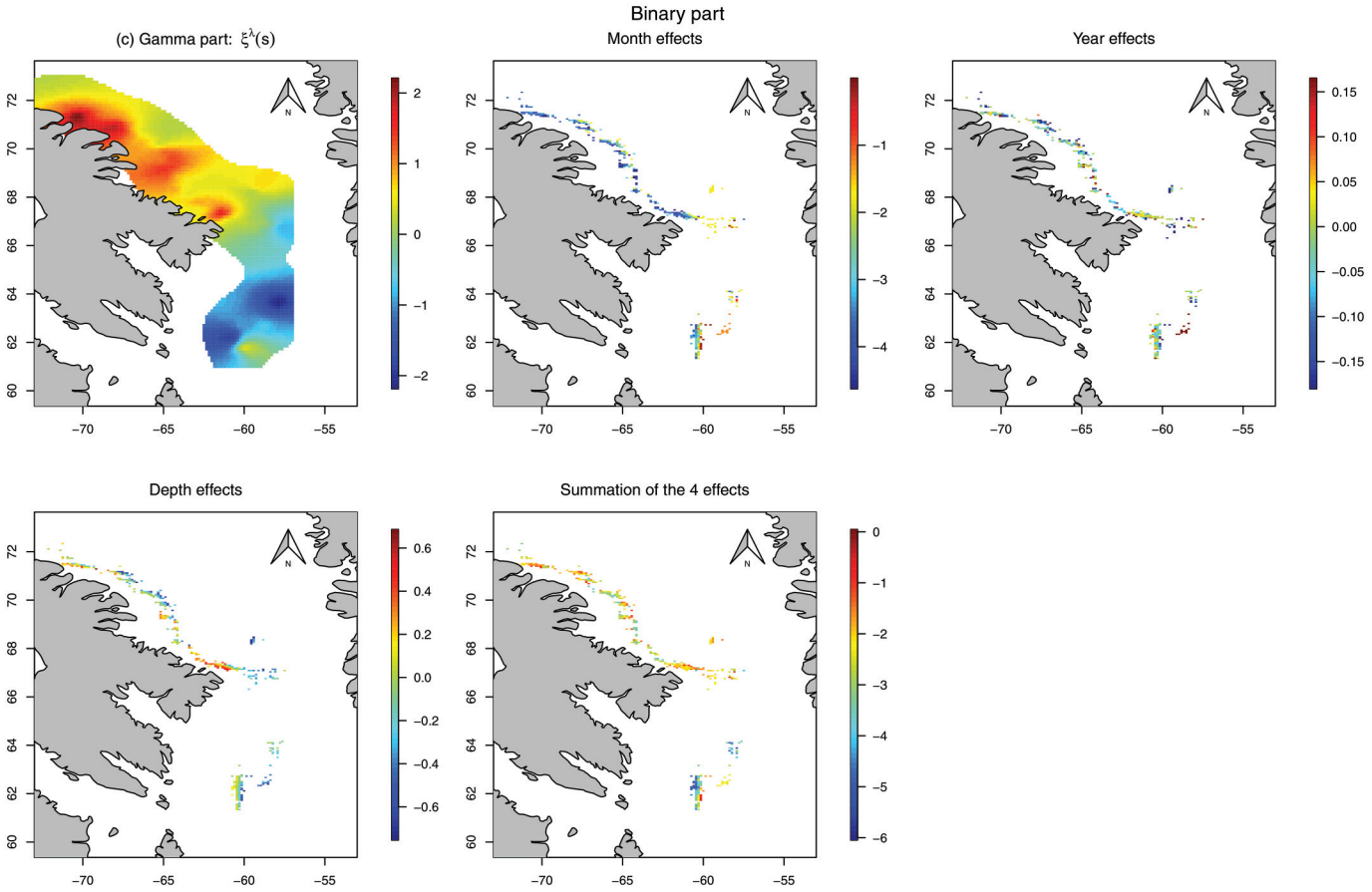

significant in both parts and the negative coefficient indicates that non-observers tend to ignore bycatch and underestimate the bycatch weights when compared with trained observers.

Figure 5 shows spatial plots of the random fields and the individual effects by month, year and depth, which are related to the underlying distribution of Greenland shark bycatch occurrence as well as their summation, at the linear predictor–logit scale for the binary part. Similarly, Fig. 6 exhibits the trip random effects, month, year and depth effects, as well as the summation of the three fixed effects in space, at the linear predictor–log scale for the gamma part, where the summation can be seen as representative of the biomass distribution of Greenland shark bycatch in space. Note that the month and year effects are at the observed time (i.e., at different month and year) and we can see months effects are clustered in space due to fishing scheme. Estimated parameters for the random effects involved in the two parts as well as the dispersion for the gamma part are presented in Table 3. For the binary part, we see an interesting spatial pattern in the random field with sporadic hotspots along the coast of Baffin Island (Fig. 5). The estimated effective range is 159 km, which implies that the spatial effects span around 159 km and above that distance the correlation becomes negligible. By comparison, the distance between the isobar 600 and 1800 m is around 50 km in the east–west direction, and the spatial random fields come into effect conditioned on depth being fitted. The weights of bycatch are distributed more erratically in space.

The month effects for both parts display some seasonal pattern but with distinct features as shown in Fig. 7. December has the highest bycatch encounter probability and bycatch weights, while September has the lowest. However, because fishing locations are not randomly sampled in different years and months (e.g., some locations are fished only in a certain month as shown by the months effects in Figs. 5 and 6), the effects in space and time could be intertwined and are therefore difficult to separate.

4. Discussion

In this study, we fitted a spatially explicit two-part model to the weights of Greenland shark bycatch in a Canadian Arctic trawl

Fig. 6. Spatial plots of the trip random effects, month, year and depth effects, as well as the summation of the fixed effects as the underlying distribution of Greenland shark bycatch magnitude on the linear predictor scale for the gamma part of the model. [Colour online.]

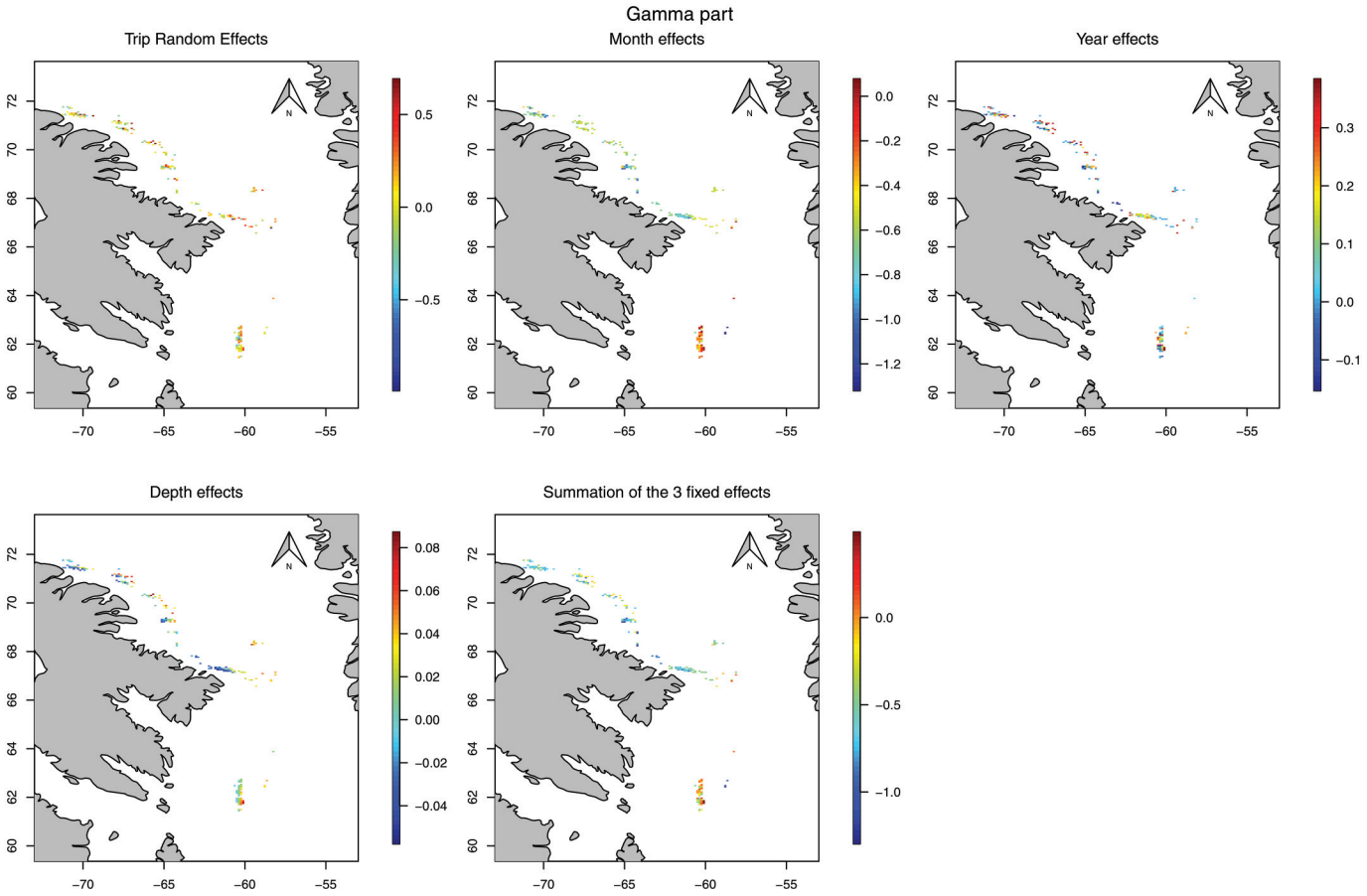

Table 3. Estimated coefficients of spatial random effects in the binary part, variance for trip random effects and dispersion parameter in gamma part.

	Binary part		Gamma part	
	Effective range	Variance σ^2	Variance σ_v^2	Dispersion σ_G^2
Estimation	159.5	1.28	0.154	0.475
SE	(59.2)	(0.50)	(0.039)	(0.022)

fishery to understand the spatiotemporal patterns and driving factors for both bycatch occurrence and magnitude. The two-part model allows us to model the bycatch occurrence probability and positive bycatch weight of Greenland shark separately with different fixed effects and spatial random effects, improving on the zero-inflated model by Cosandey-Godin et al. (2015). Our final model demonstrates some compelling spatial patterns for bycatch occurrence probability with hotspots along the coast of Baffin Island, suggesting spatially based management measures could be considered to minimize bycatch of Greenland shark in the Greenland halibut fishery. This result is consistent with observations of Greenland shark in inshore areas described by Cosandey-Godin et al. (2015) and Devine et al. (2018). The estimated effective range of the random field is 159 km, while Cosandey-Godin et al. (2015) reported a range of 175 km when analysing Greenland shark bycatch count in a Canadian Arctic gillnet fishery. Although the encounter probability of Greenland sharks is higher in the coastal area of Baffin Island, the biomass is lower than in the Northern Davis Strait. This matches the findings of Hussey et al. (2015) who reported juvenile sharks presence in North Baffin Bay fjords, which might serve as breeding or rearing areas for the sharks.

Results of the model fitting indicated that among the effects examined, month, gear and bycatch data source (observer vs non-observer) were significant. These effects can be controlled and therefore, could be candidates for management measures. Managers could consider limiting the use of twin trawls to reduce Greenland shark bycatch and ensure they have the necessary data to inform management decisions by continuing to deploy observers on fishing vessels. While interpretation of the month effect is complicated by interaction between space and time, results indicate that bycatch was higher in winter months compared to summer months, suggesting a seasonal closure could be considered to minimize bycatch.

The methods applied in this paper are relatively new and include novel features and perspectives. Most importantly, we provided Supplementary details[1] needed to make them more accessible to fisheries scientists globally. Through our model fitting procedure and our model selection decisions, we emphasize that spatial models are not a panacea for analysing datasets that contain spatial information and should not be applied blindly. Interpretability and good predictive performance are essential to be a valuable model. Therefore, researchers should proceed cautiously and always look to interpret results from a spatiotemporal model by examining parameters, and prefer those with sensible explanations for the data process.

Fig. 7. Estimated coefficients with 95% confidence intervals for year and month effects for both binary and gamma parts of the model.

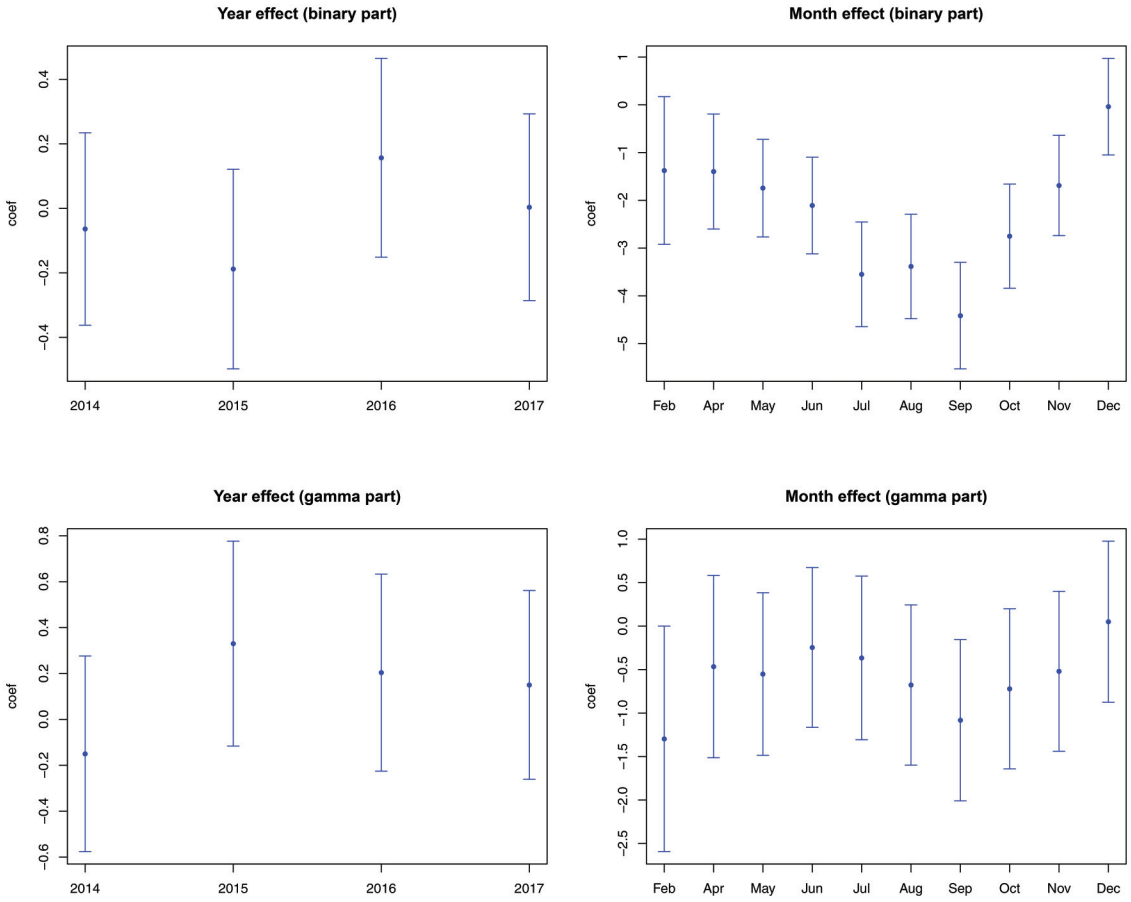

The two-part model adopted in this bycatch study can be extended in various ways for analysing bycatch data in general as outlined in the following three points. First, the spatial random effects can be extended to spatiotemporal processes if the spatial pattern differ greatly from year to year. Possible choices include random fields with autoregressive structure or summation of a consistent random field over years plus a yearly varying random field. Second, if the spatial patterns show anisotropic features (spatial correlation depends not only on the distance apart but also the direction), especially when the depth or bathymetry information is missing, the isotropic assumption for the latent random fields can be relaxed to allow for geometric anisotropy. Third, the two parts can be modelled jointly under the assumption of dependency. See Cantoni et al. (2017) for a novel correlated two-part model. Again, sometimes simple models are sufficient for analysis purposes and more complicated models should be considered only when simple models are found questionable by diagnostic plots and more complex models provide insightful information.

For future study, instead of focusing on a single bycatch species, the binary part can be extended to a multinomial model to investigate patterns for multiple bycatch species simultaneously. Also, land–sea boundaries could be taken into consideration using the barrier method (Bakka et al. 2019). The confounding problem of covariates and spatial effects we encountered deserves further study. This is a common problem when spatial random effects are added to a regression model, because covariates can also show spatial patterns, see discussion in Hodges and Reich (2010). Thaden and Kneib (2018) proposed a solution to spatial confounding by using structural equation models, where covariates are modeled jointly with the response. For example, in our bycatch data, the target weight and bycatch weight could be modelled jointly to avoid confounding. Another unique problem encountered in analysing fishery dependent data are that fishery fleets tend to go to areas known for high abundance of target species. A study on the consequences of preferential sampling on catch data analysis is welcome.

Acknowledgements

This research was carried out as part of a Collaborative Research Team Project titled “Towards Sustainable Fisheries: State Space Assessment Models for Complex Fisheries and Biological Data” led by J.M.F. and funded by the Canadian Statistical Sciences Institute (CANSSI).

References

Bakka, H., Vanhatalo, J., Illian, J., Simpson, D., and Rue, H. 2019. Non-stationary Gaussian models with physical barriers. Spatial Stat. **29**: 268–288. doi:10.1016/j.spasta.2019.01.002.

Benoît, H.P., and Allard, J. 2009. Can the data from at-sea observer surveys be used to make general inferences about catch composition and discards? Can. J. Fish. Aquat. Sci. **66**(12): 2025–2039. doi:10.1139/F09-116.

Campana, S.E., Fisk, A.T., and Klimley, A.P. 2015. Movements of Arctic and northwest Atlantic Greenland sharks (*Somniosus microcephalus*) monitored with archival satellite pop-up tags suggest long-range migrations. Deep Sea Res. Part II Top. Stud. Oceanogr. **115**: 109–115. doi:10.1016/j.dsr2.2013.11.001.

Campbell, R.A. 2004. CPUE standardisation and the construction of indices of stock abundance in a spatially varying fishery using general linear models. Fish. Res. **70**(2): 209–227. doi:10.1016/j.fishres.2004.08.026.

Cantoni, E., Flemming, J.M., and Welsh, A.H. 2017. A random-effects hurdle model for predicting bycatch of endangered marine species. Ann. Appl. Stat. **11**(4): 2178–2199. doi:10.1214/17-AOAS1074.

Carson, S., Shackell, N., and Flemming, J.M. 2017. Local overfishing may be avoided by examining parameters of a spatio-temporal model. PloS ONE, **12**(9): e0184427. doi:10.1371/journal.pone.0184427.

Cosandey-Godin, A., Krainski, E.T., Worm, B., and Flemming, J.M. 2015. Applying Bayesian spatiotemporal models to fisheries bycatch in the Canadian Arctic. Can. J. Fish. Aquat. Sci. **72**(2): 186–197. doi:10.1139/cjfas-2014-0159.

Curtis, K.A., and Carretta, J.V. 2020. Obscovgtools: assessing observer coverage needed to document and estimate rare event bycatch. Fish. Res. **225**: 105493. doi:10.1016/j.fishres.2020.105493.

Davies, R., Cripps, S., Nickson, A., and Porter, G. 2009. Defining and estimating global marine fisheries bycatch. Mar. Pol. **33**(4): 661–672. doi:10.1016/j.marpol.2009.01.003.

Devine, B.M., Wheeland, L.J., and Fisher, J.A.D. 2018. First estimates of Greenland shark (*Somniosus microcephalus*) local abundances in Arctic waters. Sci. Rep. **8**(1): 974. doi:10.1038/s41598-017-19115-x.

Gavaris, S. 1980. Use of a multiplicative model to estimate catch rate and effort from commercial data. Can. J. Fish. Aquat. Sci. **37**(12): 2272–2275. doi:10.1139/f80-273.

Graham, N., Grainger, R., Karp, W.A., MacLennan, D.N., MacMullen, P., and Nedreaas, K. 2011. An introduction to the proceedings and a synthesis of the 2010 ICES Symposium on Fishery-Dependent Information. ICES J. Mar. Sci. **68**(8): 1593–1597. doi:10.1093/icesjms/fsr136.

Griewank, A., and Walther, A. 2008. Evaluating derivatives: principles and techniques of algorithmic differentiation. 2nd ed. Society for Industrial and Applied Mathematics, Philadelphia, Pa.

Guisan, A., Edwards, T.C., and Hastie, T. 2002. Generalized linear and generalized additive models in studies of species distributions: setting the scene. Ecol. Modell. **157**(2): 89–100. doi:10.1016/S0304-3800(02)00204-1.

Hartig, F. 2020. DHARMa: Residual Diagnostics for Hierarchical (Multi-Level/Mixed) Regression Models. R package version 0.3.3.0.

Helser, T.E., Punt, A.E., and Methot, R.D. 2004. A generalized linear mixed model analysis of a multi-vessel fishery resource survey. Fish. Res. **70**(2): 251–264. doi:10.1016/j.fishres.2004.08.007.

Hodges, J.S., and Reich, B.J. 2010. Adding spatially-correlated errors can mess up the fixed effect you love. Am. Stat. **64**(4): 325–334. doi:10.1198/tast.2010.10052.

Hubert, M., and Vandervieren, E. 2008. An adjusted boxplot for skewed distributions. Comput. Stat. Data Anal. **52**(12): 5186–5201. doi:10.1016/j.csda.2007.11.008.

Hussey, N.E., Cosandey-Godin, A., Walter, R.P., Hedges, K.J., VanGerwen-Toyne, M., Barkley, A.N., et al. 2015. Juvenile Greenland sharks *Somniosus microcephalus* (Bloch & Schneider, 1801) in the Canadian Arctic. Polar Biol. **38**: 493–504. doi:10.1007/s00300-014-1610-y.

Kristensen, K., Nielsen, A., Berg, C.W., Skaug, H., and Bell, B.M. 2016. TMB: Automatic differentiation and Laplace approximation. J. Stat. Soft. **70**(5): 1–21. doi:10.18637/jss.v070.i05.

Lindgren, F., Rue, H., and Lindström, J. 2011. An explicit link between Gaussian fields and Gaussian Markov random fields: the stochastic partial differential equation approach. J. R. Stat. Soc. **73**(4): 423–498. doi:10.1111/j.1467-9868.2011.00777.x.

Lo, N.C.-H., Jacobson, L.D., and Squire, J.L. 1992. Indices of relative abundance from fish spotter data based on delta-lognormal models. Can. J. Fish. Aquat. Sci. **49**(12): 2515–2526. doi:10.1139/f92-278.

MacNeil, M.A., McMeans, B.C., Hussey, N.E., Vecsei, P., Svavarsson, J., Kovacs, K.M., et al. 2012. Biology of the Greenland shark *Somniosus microcephalus*. J. Fish Biol. **80**(5): 991–1018. doi:10.1111/j.1095-8649.2012.03257.x.

Maunder, M.N., and Punt, A.E. 2004. Standardizing catch and effort data: a review of recent approaches. Fish. Res. **70**: 141–159. doi:10.1016/j.fishres.2004.08.002.

Min, Y., and Agresti, A.A. 2002. Modeling nonnegative data with clumping at zero: a survey. J. Iran. Stat. Soc. **1**(1): 7–33. doi:10.1093/bioinformatics/bti623.

Nielsen, J., Hedeholm, R., Simon, M., and Steffensen, J. 2014. Distribution and feeding ecology of the Greenland shark (*Somniosus microcephalus*) in Greenland waters. Polar Biol. **37**(1): 37–46. doi:10.1007/s00300-013-1408-3.

Nielsen, J., Hedeholm, R.B., Heinemeier, J., Bushnell, P.G., Christiansen, J.S., Olsen, J., et al. 2016. Eye lens radiocarbon reveals centuries of longevity in the Greenland shark (*Somniosus microcephalus*). Science, **353**(6300): 702–704. doi:10.1126/science.aaf1703.

Nishida, T., and Chen, D.-G. 2004. Incorporating spatial autocorrelation into the general linear model with an application to the yellowfin tuna (*Thunnus albacares*) longline CPUE data. Fish. Res. **70**(2): 265–274. doi:10.1016/j.fishres.2004.08.008.

Ortiz, M., and Arocha, F. 2004. Alternative error distribution models for standardization of catch rates of non-target species from a pelagic longline fishery: billfish species in the Venezuelan tuna longline fishery. Fish. Res. **70**(2): 275–297. doi:10.1016/j.fishres.2004.08.028.

Pante, E., and Simon-Bouhet, B. 2013. marmap: a package for importing, plotting and analyzing bathymetric and topographic data in R. PLoS ONE, **8**(9): e73051. doi:10.1371/journal.pone.0073051. PMID:24019892.

R Core Team. 2021. R: a language and environment for statistical computing. R Foundation for Statistical Computing, Vienna, Austria. Available from https://www.R-project.org.

Rusyaev, S.M., and Orlov, A.M. 2013. Bycatches of the Greenland shark *Somniosus microcephalus* (Squaliformes, Chondrichthyes) in the Barents Sea and the adjacent waters under bottom trawling data. J. Ichthyol. **53**(1): 111–115. doi:10.1134/S0032945213010128.

Shelton, A.O., Thorson, J.T., Ward, E.J., and Feist, B.E. 2014. Spatial semiparametric models improve estimates of species abundance and distribution. Can. J. Fish. Aquat. Sci. **71**(11): 1655–1666. doi:10.1139/cjfas-2013-0508.

Shepherd, B.E., Li, C., and Liu, Q. 2016. Probability-scale residuals for continuous, discrete, and censored data. Can. J. Stat. **44**(4): 463–479. doi:10.1002/cjs.11302.

Sims, M., Cox, T., and Lewison, R. 2008. Modeling spatial patterns in fisheries bycatch: Improving bycatch maps to aid fisheries management. Ecol. Appl. **18**(3): 649–661. doi:10.1890/07-0685.1 PMID:18488624.

Sing, T., Sander, O., Beerenwinkel, N., and Lengauer, T. 2005. ROCR: visualizing classifier performance in R. Bioinformatics, **21**(20): 3940–3941. doi:10.1093/bioinformatics/bti623.

Stein, M.L. 1999. Interpolation of spatial data. Springer, New York.

Thaden, H., and Kneib, T. 2018. Structural equation models for dealing with spatial confounding. Am. Stat. **72**(3): 239–252. doi:10.1080/00031305.2017.1305290.

Thorson, J.T. 2019. Guidance for decisions using the vector autoregressive spatio-temporal (vast) package in stock, ecosystem, habitat and climate assessments. Fish. Res. **210**: 143–161. doi:10.1016/j.fishres.2018.10.013.

Thorson, J.T., and Ward, E.J. 2013. Accounting for space–time interactions in index standardization models. Fish. Res. **147**: 426–433. doi:10.1016/j.fishres.2013.03.012.

Thorson, J.T., Shelton, A.O., Ward, E.J., and Skaug, H.J. 2015. Geostatistical delta-generalized linear mixed models improve precision for estimated abundance indices for West Coast groundfishes. ICES J. Mar. Sci. **72**(5): 1297–1310. doi:10.1093/icesjms/fsu243.

Zuur, A.F., Ieno, E.N., Walker, N., Saveliev, A.A., and Smith, G.M. 2009. Mixed effects models and extensions in ecology with R. Springer-Verlag, New York.

Zuur, A.F., Ieno, E.N., and Elphick, C.S. 2010. A protocol for data exploration to avoid common statistical problems. Methods Ecol. Evol. **1**(1): 3–14. doi:10.1111/j.2041-210X.2009.00001.x.